0 0 0 0 4 2 0 1 3 9 2

Submitted to Journal of Applied Physics

LBL-3168
Preprint c.1

EVAPORATION OF SOLIDS BY LASER PULSES
PART II - ZIRCONIUM HYDRIDE

R. A. Olstad and D. R. Olander

August, 1974

Prepared for the U. S. Atomic Energy Commission
under Contract W-7405-ENG-48

For Reference

Not to be taken from this room

LAWRENCE BERKELEY LABORATORY
UNIVERSITY OF CALIFORNIA
BERKELEY

LBL-3168
c.1

DISCLAIMER

This document was prepared as an account of work sponsored by the United States Government. While this document is believed to contain correct information, neither the United States Government nor any agency thereof, nor the Regents of the University of California, nor any of their employees, makes any warranty, express or implied, or assumes any legal responsibility for the accuracy, completeness, or usefulness of any information, apparatus, product, or process disclosed, or represents that its use would not infringe privately owned rights. Reference herein to any specific commercial product, process, or service by its trade name, trademark, manufacturer, or otherwise, does not necessarily constitute or imply its endorsement, recommendation, or favoring by the United States Government or any agency thereof, or the Regents of the University of California. The views and opinions of authors expressed herein do not necessarily state or reflect those of the United States Government or any agency thereof or the Regents of the University of California.

0 0 0 0 4 2 0 1 3 9 3

EVAPORATION OF SOLIDS BY LASER PULSES
PART II - ZIRCONIUM HYDRIDE

R. A. Olstad and D. R. Olander

Inorganic Materials Research Division, Lawrence Berkeley Laboratory
and Department of Nuclear Engineering, College of Engineering;
University of California, Berkeley, California 94720

ABSTRACT

The vaporization of hydrogen from the binary solid compound zirconium hydride induced by pulses from a Q-switch ruby laser was studied using a quadrupole mass spectrometer. The rate of vaporization of H and H_2 during the rapid temperature transient was determined from the measured mass spectrometer signals.

Application of an equilibrium model to the vaporization process predicts that predominantly H_2 (rather than H atoms) should be emitted. The vaporized hydrogen should have a Maxwellian velocity distribution characteristic of the instantaneous surface temperature, and the rates of vaporization should be related to the equilibrium H_2 and H pressures by the Langmuir equation. Since the equilibrium pressure is a function of both surface temperature and surface hydrogen concentration, it was necessary to solve simultaneously the time-dependent heat conduction and hydrogen diffusion equations in the heated zirconium hydride in order to predict the vaporization rates.

It was found that H atoms and H_2 molecules were emitted at thermal equilibrium with the surface. At low laser power density, the magnitude of the H_2 signals agreed with the equilibrium model. At high laser power density, the magnitude of the H_2 signals was less than predicted, possibly because of a diffusion barrier at the surface. The H atom signals were much larger than predicted, indicating that they were produced by a non-equilibrium surface process which favored direct vaporization of adsorbed hydrogen atoms rather than recombination followed by H_2 desorption.

I. INTRODUCTION

The purpose of this investigation was to examine the vaporization behavior of a binary solid compound subjected to rapid transient heating by a pulsed laser. Most previous studies have examined the interaction of laser radiation with elemental solids (especially metals), although binary alloys and binary semiconductors have been qualitatively investigated (see references 1 - 5 in Part I). The binary compound zirconium hydride was chosen for the present study for several reasons: (a) the large partial pressure of hydrogen in equilibrium with zirconium hydride at elevated temperatures permits easy detection of the emitted particles; (b) the material properties of zirconium hydride have been studied extensively; and (c) the behavior of zirconium hydride under transient heating conditions is of interest because of its nuclear applications in TRIGA research reactors and SNAP (Systems for Nuclear Auxiliary Power) reactors.

By mass spectrometer analysis of the particles emitted from a zirconium hydride sample heated by a Q-switch laser, the following information was sought: (a) whether the hydrogen is emitted as H_2 molecules, as expected from equilibrium considerations, or whether it is emitted as H atoms; (b) whether the velocity distribution of the emitted particles is that expected for thermal equilibrium at the surface; and (c) whether the amount of emitted particles is that expected for an equilibrium process.

Although the time scale of the temperature transient is on the order of 10^{-8} seconds, heat and mass transport in the solid were analyzed by application of macroscopic conservation equations

(i.e., Fick's law and Fourier's law). The justification for using an equilibrium model of heat transport within the solid is that the time scale of the laser pulse (10^{-8} sec) is much larger than the electron collision and lattice vibration times (10^{-13} sec). Since the photons are absorbed by the electrons of the material, the photon energy should be converted to heat instantaneously. Since heat is transported by lattice vibrations and electrons, the concept of thermal conductivity should be applicable.

The validity of ordinary diffusion theory in transients lasting only 10^{-9} sec, however, is less defensible. Migration of hydrogen atoms in the zirconium matrix takes place by jumping from one interstitial position to another. Although the vibration frequency of hydrogen atoms in equilibrium sites in the solid is $\sim 10^{13}$ sec^{-1}, the jump frequency may be smaller by several orders of magnitude because of the energy barrier at the saddle point of the jump. Consequently, the average time between jumps may be of the same magnitude as the duration of the Q-switched laser pulse. Application of ordinary diffusion theory under such circumstances may not be justified.

Finally, the vaporization processes occurring at the surface may <u>not</u> be well approximated by equilibrium considerations usually applied to steady state or slow transient situations. The present investigation was directed at the surface vaporization phenomena rather than the heat and mass transport processes in the solid. Because of the close coupling of surface and bulk processes during the transient initiated by a laser pulse, the surface phenomena can be evaluated only if the transport processes in the solid are assumed to be adequately described by conventional theory.

Qualitatively, vaporization of zirconium hydride heated by a laser pulse may be described as follows: (a) the laser radiation absorbed at the surface causes a temperature transient according to the time-dependent heat conduction equation; (b) H_2 molecules and some H atoms are emitted from the heated surface at a rate which depends on surface temperature and hydrogen content of the solid at the surface; and (c) the depletion of hydrogen near the surface caused by hydrogen vaporization is partially rectified by diffusion from the interior.

The major question we wish to answer is whether the overall process is adequately described by a model based upon equilibrium vaporization from the surface coupled to the macroscopic model of heat and mass transport in the solid. Consequently, only the effect of low energy laser pulses was investigated in this study. The vaporization of the zirconium component and production of an ionized plume of vapor, which occur at high laser power densities, were not of interest; some data pertinent to these processes are presented in reference 6 of Part I.

II. EXPERIMENTAL

The system described in the previous paper (Part I) is employed in the present investigation. Because of the high hydrogen pressure in equilibrium with heated zirconium hydride, detectable H_2 and H signals could be obtained for Q-switched laser pulses containing less than 0.1 J energy. The Q-switched pulses exhibit the temporal shape of an isosceles triangle. This time dependence is described by Eq. (2) of Part I with the peak occurring at τ_1 = 40 nsec and the pulse terminating at τ_2 = 80 nsec.

The lens used for focusing the laser beam on the target has a focal length of 100 cm, so that the parameter characterizing the size of the beam spot, σ, is 0.26 cm, or the beam spot is $\sim$ 0.5 cm in diameter. Since the rods of zirconium hydride used as targets are 0.32 cm in diameter, the radial variation of power density in the laser is not important. In the present series of experiments, the centerline laser intensity (Eq. (1) of Part I with $r = 0$) adequately describes the power density over the entire target.

The targets were fabricated by hydriding high purity zirconium rods 0.32 cm in diameter using the combination of hydrogen pressure and temperature needed to produce the compound $ZrH_{1.63}$. This particular hydrogen-to-metal ratio was chosen because the δ-hydride structure is preserved from room temperature to > 1000°C (Figure 1). The end of the zirconium hydride rod was polished with 6 micron diamond paste and mounted on the end of the linear feedthrough in the target chamber. After each laser shot on the end, the rod was removed and repolished before firing on it again.

Since the emissivity of the surface is important in the theoretical analysis, the reflectivity of the fabricated hydride was determined at room temperature. A He-Ne gas laser was directed at the surface and the ratio of the intensities of the incident and reflected beams was determined using a photomultiplier. The reflectivity was found to be 0.45 ± 0.05 at the He-Ne laser wavelength. This value probably applies to the ruby laser wavelength as well. However, it is valid only for the polished surface and most probably is not applicable to the roughened hot surface created by pulsing with intense laser beams.

We did not attempt to produce a steady molecular beam of H_2 in order to calibrate the mass spectrometer for this species. Instead, the instrumental constant K (Eq. (3) of Part I) was determined by simultaneously measuring the mass spectrometer output signal and the pressure of H_2 added to the mass spectrometer chamber. After correcting the ion gauge reading to obtain the true hydrogen pressure, the density of H_2 molecules was calculated from the ideal gas law and the instrumental constant was obtained by dividing the molecular density into the mass spectrometer signal. This method of calibrating the mass spectrometer is not as accurate as the technique based upon passing a molecular or atomic beam of known strength through the ionizer, as was done in Part I for calibration of the detector for iron. However, calibration based upon random background gas is probably accurate to within a factor of two or three even though the desired signal in the experiment arises from a molecular beam of H_2 passing through the ionizer.

The instrumental constant for atomic hydrogen was obtained by correcting the measured value for molecular hydrogen for the ratio of the ionization cross sections and the estimated numbers of secondary electrons produced at the first dynode of the electron multiplier. These corrections approximately cancel each other, so that the sensitivities of the mass spectrometer to atomic and molecular hydrogen are about equal. For the mass spectrometer settings used, a value $K = 1.5 \times 10^{-15}$ amps-cm^{-3} was deduced.

Transient mass spectrometer signals were processed to determine n(t) by use of Eq. (5) of Part I. In this equation, $t_d = 3$ μsec

for H^+ and 4 μsec for H_2^+. For the circuitry employed in the detection of hydrogen signals, the RC time constant τ was 12 μsec.

III. RESULTS

Figure 2 shows the output signal of the mass spectrometer set to detect H_2^+ following a Q-switched laser pulse on $ZrH_{1.63}$. Figure 3 shows the molecular density pulse n(t) determined from the output signal S(t) after using the correction procedure embodied in Eq. (5) of Part I. The correction results in narrowing the pulse and displacing the peak towards time zero. Table 1 presents the characteristics of the molecular pulse for laser pulses of various energies. In the nomenclature of Part I, FWHM is equal to $t_{1/2}^+ - t_{1/2}^-$. For pulses of 0.25 J energy or greater, energetic H^+ and Zr^+ ions were emitted from the target and were identified by mass spectrometer detection with the ionizer turned off. The data reported under Series A and B in Table 1 were taken about a month apart under slightly different conditions (e.g., different flashlamps and different laser alignment). Atomic hydrogen signals were measured in a third series of experiments. The H^+ signals were quite substantial and could not be confounded with signals due to fragmentation or double ionization of H_2.

IV. THEORY OF EQUILIBRIUM VAPORIZATION OF ZIRCONIUM HYDRIDE DURING A LASER PULSE

A. Surface Temperature and Surface Hydrogen Concentration

As explained in the introduction, the macroscopic conservation equations for both heat and mass must be solved when the response of a binary solid struck by a laser pulse is analyzed. The energy equation is similar to Eq. (6) of Part I. In addition, however, the

diffusing species (atomic hydrogen) transports energy, and according to the theory of irreversible thermodynamics, the existence of a concentration gradient implies a flux of energy (the Dufour effect). These two contributions appear in the energy equation. Because the mass of hydrogen is small compared to that of essentially non-volatile zirconium, the convective term due to surface recession may be neglected. With these modifications, the energy equation becomes:

$$\rho C_v \frac{\partial T}{\partial t} = \frac{\partial}{\partial x}\left[DQ^* N_{Zr} \frac{\partial y}{\partial x} + \kappa \frac{\partial T}{\partial x}\right] + DN_{Zr}\left[\frac{\partial y}{\partial x} + \frac{Q^* y}{RT^2}\frac{\partial T}{\partial x}\right]\frac{\partial \overline{H}_H}{\partial x} \tag{1}$$

where ρC_v and κ are the heat capacity per unit volume and the thermal conductivity, respectively, of zirconium hydride. D is the diffusion coefficient of hydrogen in the solid and Q* is the heat of transport. N_{Zr} is the number of zirconium atoms per unit volume, R is the gas constant and $\overline{H}_H$ is the partial molar enthalpy of hydrogen in zirconium hydride. y is the H/Zr atom ratio, which is determined by the diffusion equation:

$$\frac{\partial y}{\partial t} = \frac{\partial}{\partial x}\left[D\frac{\partial y}{\partial x} + \frac{DQ^* y}{RT^2}\frac{\partial T}{\partial x}\right] \tag{2}$$

In deriving Eqs. (1) and (2), the zirconium atoms are represented by a fixed, rigid lattice through which the hydrogen migrates as atoms from the bulk to the surface where recombination to form H_2 and vaporization occurs. The energy and diffusion equations are coupled and need to be solved simultaneously. No useful analytic solutions are available, so numerical solutions were obtained by computer.

The initial conditions are:

$$T(x,0) = T_o \quad ; \qquad y(x,0) = 1.63 \tag{3}$$

The boundary conditions far from the surface are:

$$T(\infty,t) = T_o \quad ; \qquad y(\infty,t) = 1.63 \tag{4}$$

The thermal boundary condition at the surface (analogous to Eq. (9) of Part I) is:

$$-\left[\kappa - \frac{D\ Q^{*2}\ N_{Av}\ y_s}{RT_s^2}\right]\left(\frac{\partial T}{\partial x}\right)_0 = -\ 2\Phi(T_s,y_s)(\Delta H_{vap} - Q^*) - \varepsilon\sigma_s(T_s^4 - T_o^4) + q(t) \tag{5}$$

where $T_s = T(0,t)$ and $y_s = y(0,t)$ are the surface temperature and surface H/Zr atom ratio, respectively. $\Phi(T_s,y_s)$ is the rate of vaporization of molecular hydrogen from the surface as calculated by Eq. (10) of Part I with the appropriate changes in P and M. ΔH_{vap} is the heat of vaporization per gram atom of H. $q(t)$ is the heat flux from the laser which is given by Eqs. (11) and (12) of Part I. As noted in the Introduction, the radial variation of q is not significant in the present experiments because of the large beam spot, so that $\exp(-\ r^2/\sigma^2) \simeq 1$.

The surface boundary condition for the diffusion equation is:

$$-\ D\left(\frac{\partial y}{\partial x}\right)_0 = -\ \frac{2\Phi(T_s,y_s)}{N_{Zr}} - \frac{D\ Q^*\ y_s}{RT_s^2}\left(\frac{\partial T}{\partial x}\right)_0 \tag{6}$$

B. H_2 Density in the Ionizer

The quantity to be compared with the data, n(t), is given by Eq. (18) of Part I with the following modifications: (i) the vapor pressure $P(T_s)$ is replaced by the equilibrium pressure of atomic or molecular hydrogen which are functions of both T_s and y_s; (ii) m represents the mass of H or H_2; (iii) the effective spot size, A_{eff}, is set equal to the area of the end of the zirconium hydride rod because the laser spot is larger than the target cross sectional area; (iv) the calculated density is multiplied by the peaking factor to account for the fact that the pulsed molecular beam does not occupy the entire ionizer of the mass spectrometer as does the random background gas upon which this instrument was calibrated. The peaking factor χ is calculated to be approximately 0.44 for the geometry of our system. The final expression for n(t) is:

$$n(t) = \chi A_{rod} \frac{\ell}{k}\left(\frac{m}{2\pi k}\right)^{3/2} \int_0^t \frac{P(T_s,y_s)}{T_s^{5/2}(t-\tau)^4} \exp\left\{-\frac{m\ell^2}{2kT_s(t-\tau)^2}\right\} d\tau \qquad (7)$$

where A_{rod} is the area of the zirconium hydride target. The surface temperature and hydrogen concentration depend upon time variable τ and the peak heat flux q_p, although these symbols have been omitted for clarity. For want of any data, the condensation coefficient α is assumed to be unity.

C. Thermochemical Properties of Zirconium Hydride

Theoretical prediction of the density pulse n(t) requires thermodynamic information on the H_2 pressure in equilibrium with ZrH_n ($n \leq 1.63$) as a function of temperature and composition. In

addition, the heat of vaporization and the partial molar enthalpy $\overline{H}_H$ are needed for the thermal analysis.

Zirconium is an exothermic absorber of hydrogen which forms solid solutions and hydrides of varying composition depending on temperature and hydrogen content. The alpha and beta phases (Figure 1) are low and high temperature solid solutions of hydrogen in alpha and beta zirconium, respectively. The latter consists of zirconium atoms on a body-centered cubic lattice with the H atoms in solid solution. The delta and epsilon phases are hydride phases with maximum hydrogen content at the stoichiometric composition ZrH_2. Neutron diffraction studies have shown that the delta phase has a fluorite structure with the zirconium atoms on a face-centered cubic lattice and the hydrogen atoms in tetrahedral sites (1).

If the behavior of the zirconium hydride during the laser-induced temperature transient were truly an equilibrium process, the phase structure at all times would be given by the phase diagram of Figure 1. As the δ-phase hydride heats up, vaporization from the surface depletes the hydrogen concentration. When the temperature and hydrogen concentration place the system on the $\delta/(\beta + \delta)$ boundary, further depletion of hydrogen brings the material into the $\beta + \delta$ two-phase region. δ-phase hydride is converted to β-phase until all of the former is consumed. Still further hydrogen depletion moves the system into the β-phase region.

In order for this <u>total equilibrium</u> model to be valid, the δ- to β-phase transition would have to occur in times the order of 10^{-8} seconds, which is many orders of magnitude smaller than times required for normal phase changes. In the process of changing from

δ- to β-phase, the zirconium lattice must rearrange from the fcc to the bcc structure and the hydrogen must redistribute so that the beta phase has a low hydrogen concentration. It is possible, but not probable, that these changes could take place in such a short time; experiments on pulse-heating of zirconium-uranium hydride rods have shown that the δ- to β-phase change can occur at least in times on the order of 10^{-1} sec (2).

If the temperature transient is too rapid for the phase change to occur, the solid retains the δ-phase configuration but with hydrogen content lower than that given by the equilibrium phase diagram. Material and thermodynamic properties for this case are extrapolated from known values in the δ-phase. This model of the system is called quasi-equilibrium because the phase structure is not that given by the equilibrium phase diagram for hydrogen contents below the δ/(β + δ) boundary but the hydrogen pressure is that in equilibrium with the δ-hydride, which may or may not be subsaturated with hydrogen. The quasi-equilibrium model is probably not valid for hydrogen concentrations appreciably below that at the δ/(β + δ) boundary. For hydrogen concentrations well into the two-phase region of Figure 1, partial collapse of the metastable δ-phase to the stable beta zirconium lattice would probably occur.

The equilibrium H_2 pressure over single phase zirconium hydride may be expressed in the form:

$$\ln P_{H_2} = a(y) + b(y)/T \qquad (8)$$

where a(y) and b(y) are polynomials in the H/Zr atom ratio. Simnad and Dee (3) report the coefficients in these polynomials for the

δ-phase and the β-phase data of Beck and Mueller (1) may be fitted to the same form. The hydrogen pressures over the β + δ two-phase region may be expressed in simple Arrhenius form. For $y < 0.1$, Sievert's law (i.e., $P_{H_2} \alpha y^2$) is obeyed. Figure 4 shows the H_2 pressures used in the calculations based upon the total equilibrium model. In order to obtain the hydrogen pressure in equilibrium with subsaturated δ-phase required in the quasi-equilibrium model, the pressure in the stable δ-phase region was extrapolated to compositions which at equilibrium would be in the β + δ region of the phase diagram. Figure 5 shows the pressure-composition isotherms constructed for calculations based upon the quasi-equilibrium model.

In single phase regions, the partial molar enthalpy and the heat of vaporization are obtained from the relation:

$$\Delta H_{vap} = -\left(\overline{H}_H - \frac{1}{2} H^{\circ}_{H_2}\right) = -\frac{1}{2} R \left[\frac{\partial \ln P_{H_2}}{\partial (1/T)}\right]_y \qquad (9)$$

which may be obtained from Figures 4 or 5. $H^{\circ}_{H_2}$ is the standard molar enthalpy of H_2. Absolute values of this quantity are not needed, since only the derivative of $\overline{H}_H$ with respect to x appears in Eq. (1). $\overline{H}_H$ and ΔH_{vap} in the two-phase region of the total equilibrium model are obtained from the single-phase data by application of the lever rule. ΔH_{vap} is of the order of 20 kcal/mole.

The hydrogen diffusion coefficients in the solid have been taken as:

$$D_\delta = 5.0 \times 10^{-3} \exp\left(-\frac{12.3}{R(T/10^3)}\right) \text{cm}^2/\text{sec}$$

for the δ-phase and

$$D_\beta = 5.3 \times 10^{-3} \exp\left(-\frac{8.3}{R(T/10^3)}\right) \text{ cm}^2/\text{sec}$$

in the β-phase. The corresponding heats of transport are Q^*_δ = 1.3 kcal/mole and Q^*_β = 9 kcal/mole. The sources of these and other properties of zirconium hydride used in the calculations are discussed in detail in reference 6 of Part I.

The calculated response of the system to pulses of varying energies is shown in Figures 6 - 9. The equilibrium H_2 pressure obtained from Figure 4 (the total equilibrium model) was utilized in preparing these plots. Because the energy consumed by hydrogen vaporization is much smaller than the input heat flux from the laser, the surface temperature curves in Figure 6 do not bunch up at high power densities as they did for iron. In effect, only the first term on the left hand side and the last term on the right hand side of Eq. (5) are significant in the surface heat balance.

The H/Zr atom ratio at the surface as a function of time is shown in Figure 7 for various peak heat fluxes. For $q_p > \sim 3 \times 10^6$ watts/cm^2, substantial depletion of hydrogen occurs at the surface. The surface H/Zr ratio profiles pass through a minimum at approximately the same time as the maximum surface temperature is attained. Thereafter, the surface H/Zr ratio increases because H diffuses from the bulk to the surface faster than H_2 is lost by vaporization. The final H/Zr ratio is "frozen" at a value less than the initial value because vaporization and diffusion of hydrogen become negligible as the temperature returns to ambient.

As shown in Figure 8, the H_2 flux from the surface is a very sharp function of time, indicating that the emission occurs over a

relatively narrow temperature range (on the order of several hundred °C). The largest H_2 flux occurs when the equilibrium H_2 pressure at the surface is a maximum. This peak occurs before the maximum temperature is reached because the H_2 vapor pressure is a function of both temperature and H/Zr atom ratio.

Typical calculated mass spectrometer H_2 signals are shown in Figure 9. According to Figure 8, the H_2 molecules are emitted from the surface over a time interval of less than 0.1 μsec whereas the time of flight of the H_2 molecules from the zirconium hydride sample to the mass spectrometer ionizer is approximately 100 μsec. Therefore the H_2 molecules are emitted effectively as an instantaneous source at zero time and the width of the calculated signal is then due entirely to the spread of velocities of the emitted H_2 molecules. As energy density increases, the calculated signal shifts toward the origin because of the increase in the velocity of the emitted molecules due to the higher surface temperature. There is a time delay of approximately 30 μsec between the time the molecules are emitted from the surface and their arrival at the ionizer because of the time required for the molecules in the high speed tail of the Maxwell-Boltzmann distribution to traverse the 40 cm separating these two locations.

Although temperature gradients at the surface reach values greater than 10^7 °C/cm, the Soret effect and the effect of the enthalpy transported by the diffusing hydrogen atoms are both negligible. The numerical solution of the solid energy equation and hydrogen diffusion equation (Eqs. (1) - (6)) were made with the heat of transport (Q*) and the gradient of the partial molar

enthalpy of hydrogen $\left(\frac{\partial \bar{H}_H}{\partial x}\right)$ set to zero. Each deletion made a less than 10% difference on the magnitude of the predicted signal (n_{max}) and had negligible influence on t_{peak} and FWHM.

If the vaporization process is adequately described by equilibrium thermodynamics, the hydrogen emitted from the surface during the laser pulse should contain a small proportion of H atoms along with the preponderant molecular form. The predicted atom hydrogen density pulse at the ionizer may be obtained from Eq. (7) with m equal to the mass of an H atom and with the pressure of atomic hydrogen obtained from the equilibrium H_2 pressure by:

$$P_H = K_p \sqrt{P_{H_2}} \tag{10}$$

where K_p is the equilibrium constant for hydrogen dissociation in the gas phase ($\frac{1}{2} H_2(g) = H(g)$). The predicted ratio $(n_{max})_H/(n_{max})_{H_2}$ varies from 10^{-7} to 10^{-3} as the peak heat flux ranges from 4×10^6 to 10^7 watts/cm^2. For a fixed peak power, the average velocity of the H atoms should be $\sqrt{2}$ times greater than the H_2 velocity, so that the peak of the number density pulse in the ionizer should occur 30% sooner for H than for H_2.

V. COMPARISON OF THEORY AND EXPERIMENT

Complete comparison of theory with experiment requires that surface emmisivity be known in order to relate pulse energy to peak heat flux according to Eq. (17) of Part I. To eliminate the uncertainty in ε (and in the magnitude of E as well), we have constructed plots of t_{peak} vs FWHM (Figure 10) which should be independent of surface emissivity. Since the molecules are emitted

over a time much less than t_{peak}, the ratio t_{peak}/FWHM is characteristic only of the velocity distribution of the emitted molecules. Although the data are scattered, they cluster about the straight line representing the calculated variation of t_{peak} vs FWHM for a Maxwellian beam. This indicates that the H_2 molecules and H atoms are emitted with the velocity distribution of an effusive Maxwellian source.

The calculated and experimental values of arrival time vs pulse energy are plotted in Figure 11. The H_2 data points cluster about the theoretical curve for a surface emissivity of unity, although the scatter is too great to decide whether the equilibrium model or the quasi-equilibrium model is more appropriate. The theoretical H_2 curve for $\varepsilon = 0.55$ is clearly out of the range of the data points. The apparent surface reflectivity is therefore approximately equal to zero, rather than 0.45 as measured with the He-Ne laser on room temperature $ZrH_{1.63}$. The reflectivity during a Q-switch pulse may be much less than the measured reflectivity either because the zirconium hydride reflectivity may be very small at high temperatures, or because the change in surface condition during the vaporization process may cause the reflectivity to be very small. Several experiments on metals using conventional mode pulses (4,5) and Q-switched pulses (6) have shown that the surface reflectivity during a laser pulse can be much less than the initial reflectivity.

Notwithstanding the uncertainty in ε, the agreement between the measured and calculated values of t_{peak} vs E shown in Figure 11 indicates that the emitted H_2 molecules are in thermal equilibrium

with the surface. The surface temperature is apparently calculated correctly from the simultaneous solution of the energy and mass transport equations in the binary solid.

Figure 11 shows that the values of t_{peak} for H atoms are substantially smaller than t_{peak} for H_2 at the same pulse energy, which indicates that the former signals are due to H atoms emitted from the surface rather than from cracking or double ionization of H_2. The atomic hydrogen data fall between the calculated curves for $\varepsilon = 1$ and $\varepsilon = 0.55$, which suggests that the H atoms are emitted at a somewhat lower temperature than the H_2 molecules.

The calculated and measured values of the molecular density in the ionizer at the peak of the pulse are plotted in Figure 12. The three H_2 data points with n_{max} much less than the band drawn through the other H_2 points are attributed to misalignment of the laser on the surface so that the actual incident energy density was smaller than measured by the photodiode. The band through the remaining H_2 data agrees fairly well with the calculated curve for $\varepsilon = 1$ for E less than 0.05 joules. However, for E greater than this value, the measured values of $(n_{max})_{H_2}$ saturate at $\sim 10^9$ molecules/cm^3 while the calculated values increase to $> 10^{10}$ molecules/cm^3. The slope of the calculated curve is steep at low energies because the equilibrium hydrogen pressure in this region is primarily a function of temperature. As the laser energy increases, the slope decreases because hydrogen is depleted from the surface. The theoretical $(n_{max})_{H_2}$ vs E curve therefore levels off because the H_2 flux from the surface is limited by the rate at which hydrogen can diffuse to the surface.

The theory developed in Section IV permits calculation of the yield per pulse, defined as the quantity of hydrogen escaping from a unit area of surface for a laser pulse of prescribed energy. For pulses of $\sim$ 0.1 J energy, the yield corresponds to the hydrogen content of 7 monolayers of $ZrH_{1.63}$. The hydrogen required to supply this yield has to diffuse from many lattice spacings within the solid. As indicated in the Introduction, the H atom jumping process may not be rapid enough to permit application of Fick's law to the transient mass transport phenomenon occurring as a result of the Q-switched laser pulses. The observed failure of the equilibrium vaporization theory for H_2 evident in Figure 12 at high laser powers may be due to the inadequacy of the solid state diffusional analysis in the theory.

In addition to the possible failure of macroscopic diffusion theory because of the time scale of the heating process, several other more mundane phenomena could restrict the supply of H atoms to the surface:

(a) A diffusion barrier (e.g., an oxide or nitride coat) on the surface.

(b) Restructuring of the hydrogen-depleted surface to form one of the metallic phases may result in an interface which restricts migration of H atoms to the surface.

(c) Even in the absence of diffusion barriers such as those in (a) and (b) above, there may be a kinetic barrier at the surface if the time for an H atom in the lattice to hop from just beneath the surface to a surface site is significantly greater than the time for an H atom to jump from one lattice site to another.

In each of the above cases, a surface barrier acts to reduce the flow of H atoms to the surface even though bulk diffusion is normal. Surface resistances of the types described above have often been identified from conventional kinetic studies of hydrogen permeation through metal foils (7). At the very high surface particle fluxes developed in the transient induced by laser pulsing, surface resistances assume even greater importance than in ordinary permeation experiments.

The possibility that the discrepancy in the predicted and observed H_2 signals in Figure 12 may be due to a condensation coefficient very much smaller than unity does not seem likely for the following reasons: (a) the agreement between the measured and calculated values of $(n_{max})_{H_2}$ is adequate for pulses of $E < 0.05$ J (in fact the theory underpredicts the molecular pulse). This accord indicates that $\alpha = 1$ is a satisfactory approximation for low energy pulses. (b) If the constant value of $(n_{max})_{H_2}$ observed for $E > 0.05$ J were due to a temperature-dependent condensation coefficient, this quantity would have to decrease in inverse proportion to the equilibrium hydrogen pressure, which is highly unlikely.

The measure values of the maximum density of the atomic hydrogen pulse emitted from the surface are also shown in Figure 12. In the plateau region of $E > 0.05$ J, the data indicate that the ratio of the peak amplitudes of the H to the H_2 pulses is ~ 0.2 whereas the equilibrium calculation of Section IV predicts that this ratio should be $\sim 10^{-3}$ for $E = 0.1$ J. The equilibrium theory fails rather dramatically on this point. The large H atom signals are

due to lack of attainment of chemical equilibrium at the surface, even though hydrogen atoms are emitted at thermal equilibrium with the surface (i.e., their velocity distribution is consistent with the calculated surface temperature). However, existence of thermal equilibrium does not imply chemical equilibrium. For example, the translational temperature of a supersonic nozzle beam of diatomic molecules may be quite different from the equivalent temperature of the vibrational or rotational modes of the beam molecules.

The yield of atomic hydrogen detected in the experiments amounted to less than a monolayer of H atoms in the target surface, which suggests that the H atom signal detected by the mass spectrometer may have been due to vaporization of a loosely bound adsorbed layer of H atoms in the surface of the zirconium hydride rather than hydrogen which was truly part of the zirconium hydride structure. This adsorbed layer of hydrogen may have been driven off early in the pulse thereby accounting for the slightly lower temperature of atomic hydrogen compared to that of molecular hydrogen inferred from Figure 11.

Whether the atomic hydrogen detected in the experiment arose from an adsorbed layer initially on the surface or from hydrogen reaching the surface by diffusion from the bulk solid, equilibrium thermodynamics nevertheless requires that most of the hydrogen should have evaporated as H_2 rather than H. However, the surface temperature transient may simply have been too rapid for hydrogen atoms initially present in or on the solid to recombine and form H_2 before vaporization. If the adsorbed hydrogen atoms must surface diffuse and collide with another adsorbed H atom in order to

form surface H_2 which then desorbs, the rapidity of the temperature rise may make it more likely that the H atoms simply desorb as atoms before recombination occurs. The model therefore attributes the excessive atomic hydrogen emission from the surface to the sluggishness of the reaction:

$$2H(ads) \rightarrow H_2(g)$$

compared with the direct desorption step:

$$H(ads) \rightarrow H(g)$$

At true equilibrium, or in slow transients which can be regarded as a sequence of equilibrium stages, the rates of the above two reactions are related by the requirement of detailed balancing, a condition which evidently fails in transients of a few tens of nsec. Nothing in the H-atom emission model just described prevents the atomic hydrogen from being in thermal equilibrium from the surface to which it is bound; only chemical equilibrium with respect to H_2 emission is violated.

VI. CONCLUSIONS

The conclusions of this study of hydrogen evaporation from zirconium hydride rapidly heated by Q-switched laser pulses may be summarized as follows:

(1) Both H and H_2 are emitted from the surface with Maxwell-Boltzmann velocity distributions characteristic of the instantaneous surface temperature. The latter appears to be adequately calculated from macroscopic heat conduction theory.

(2) The quantities of H and H_2 emitted during the transient do not represent chemical equilibrium, either between the atomic and molecular forms of gaseous hydrogen or between the gas phase and the calculated surface composition. For laser pulses > 0.05 J, less H_2 is emitted than predicted by the theoretical model based upon Langmuir vaporization and Fickian diffusion; for all energy pulses, more H is emitted than expected from equilibrium vaporization. The failure of the theory in these two aspects appears to arise from independent kinetic phenomena; H_2 emission would be depressed by the excessively large direct release of atomic hydrogen from the surface, but not by the order of magnitude seen from Figure 12. The explanation of abnormally low H_2 release based upon restricted migration of hydrogen from the bulk solid is not incompatible with the model of nonequilibrium atomic hydrogen desorption which has been advanced to explain the abnormally large H/H_2 ratios observed by the detector.

Finally, we note that the temperature transient initiated by the Q-switched laser pulse (duration $\sim 10^{-8}$ sec) is very much more rapid than that attainable by flash filament (8) or any other transient heating technique. Kinetic limitations which are not observable in slower transients figure prominently in vaporization by Q-switched laser pulses.

This work was done under the auspices of the U. S. Atomic Energy Commission.

0 0 0 0 4 2 0 1 4 0 5

REFERENCES

1. R. L. Beck and W. M. Mueller in "Metal Hydrides" (W. M. Mueller, J. B. Blackledge and G. G. Libowitz, Eds.), Chapter 7, Academic Press (1968).

2. R. E. Taylor, in "Compounds of Interest in Nuclear Reactor Technology",(J. T. Waber, P. Chiotti and W. N. Miner, Eds.), p. 641, AIME (Nuclear Metallurgy Vol. X) (1964).

3. M. T. Simnad and J. B. Dee, in "Thermodynamics of Nuclear Materials", (IAEA), p. 513 (1968).

4. M. K. Chun and K. Rose, J. Appl. Phys. 41, 614 (1970).

5. A. M. Bonch-Bruevich et al., Sov. Phys. - Tech. Phys. 13, 640 (1968).

6. N. G. Basov et al., Sov. Phys. - Tech. Phys. 13, 1581 (1969).

7. R. Ash and R. M. Barrer, Phil. Mag. 47, 1197 (1959).

8. D. L. Adams, L. H. Germer and J. W. May, Surf. Sci. 22, 45 (1970).

TABLE 1

Results of Mass Spectrometer Analysis of Hydrogen Signals from Q-Switch Pulses on $ZrH_{1.63}$

E (joules)	t_{peak} (μsec)	FWHM (μsec)	$n_{max} \times 10^{-9}$ (molecules/cm^3)
		H_2 (Series A)	
0.034	102.0	83.9	0.6
0.046	94.0	81.7	1.2
0.069	82.0	47.8	1.2
0.028	105.0	75.3	0.3
0.029	102.5	83.2	0.4
0.11	75.5	65.3	1.3
0.15	55.2	65.2	1.1
		H_2 (Series B)	
0.12	62.0	80.4	0.7
0.14	78.4	117.0	0.8
0.19	90.0	101.0	1.4
0.045	100.0	90.0	0.1
0.073	76.0	69.8	0.2
0.069	84.0	92.4	0.1
0.11	86.0	82.0	0.3
0.10	84.0	63.8	1.0
0.71	104.0	67.5	0.7
0.16	84.0	78.8	2.0
		Atomic Hydrogen (H)	
0.061	59.0	47.4	0.24
0.10	67.0	50.0	0.26
0.13	57.0	48.2	0.30
0.13	52.0	57.7	0.16

FIGURE CAPTIONS

Figure 1 Zirconium-hydrogen phase diagram (reference 1).

Figure 2 Typical measured H_2 signal. Horizontal scale is 20 μsec/div.

Figure 3 Typical measured and corrected H_2 signals for pulse energy of 0.12 J.

Figure 4 H_2 pressure-composition isotherms for zirconium-hydrogen system, total equilibrium model.

Figure 5 H_2 pressure-composition isotherms, quasi-equilibrium model.

Figure 6 Calculated time dependence of the surface temperature (T_s) for laser pulses of varying energy densities.

Figure 7 Calculated time dependence of the surface H/Zr atom ratio (y_s).

Figure 8 Calculated relative flux of H_2 molecules vaporized from the surface [$\Phi(T_s,y_s)$].

Figure 9 Calculated H_2 density pulse at mass spectrometer ionizer [n(t)].

Figure 10 Comparison between calculated and experimental t_{peak} vs FWHM.

Figure 11 Comparison between calculated and experimental t_{peak} vs E, for Zr-H.

Figure 12 Comparison between calculated and experimental $(n_{max})_{H_2}$ vs E.

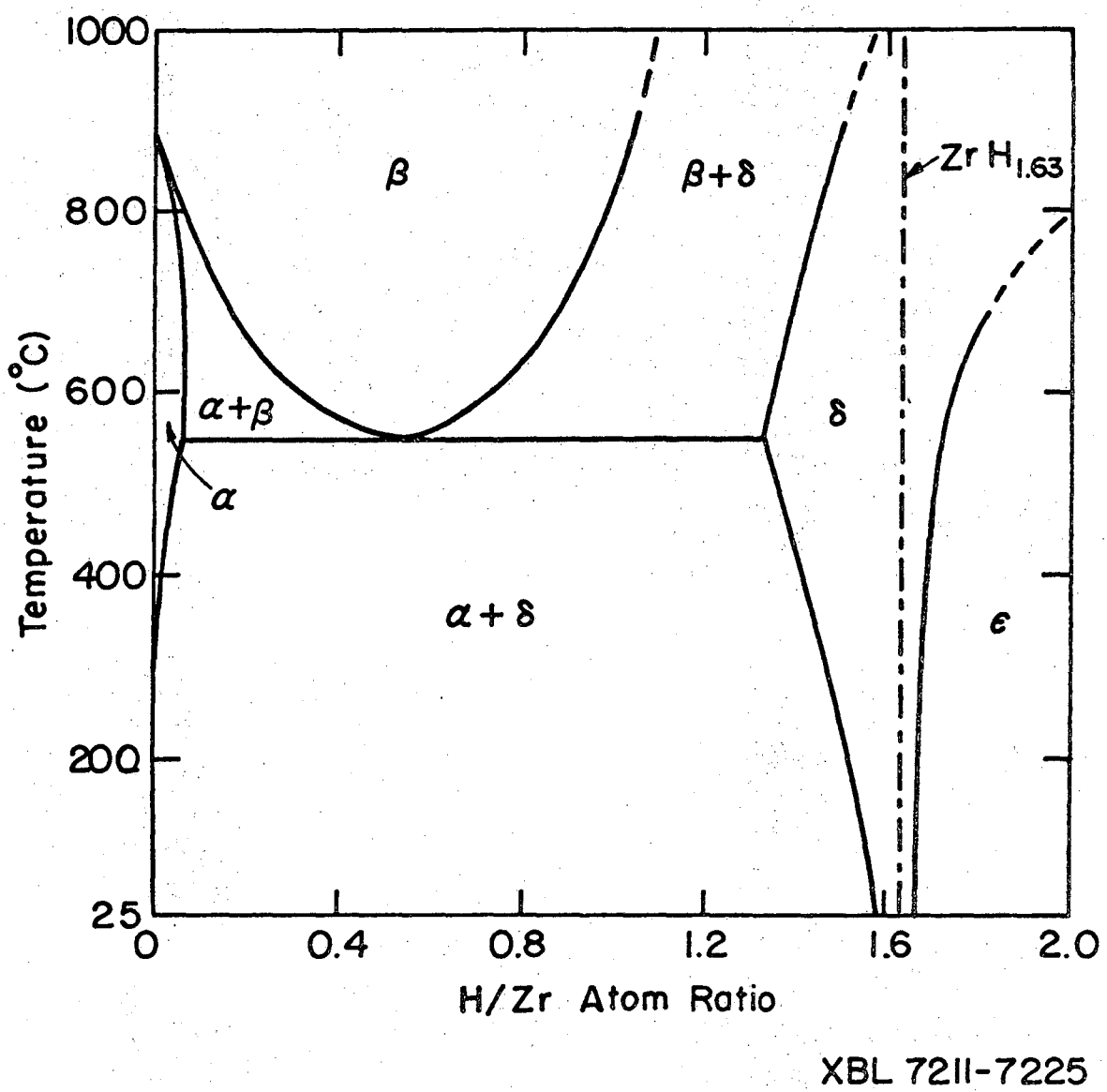
1000
800
600
400
200
25
Temperature (°C)
0
0.4
0.8
1.2
1.6
2.0
H/Zr Atom Ratio
β
β+δ
Zr H1.63
α+β
α
δ
α+δ
ε
XBL 7211-7225

Fig. 1

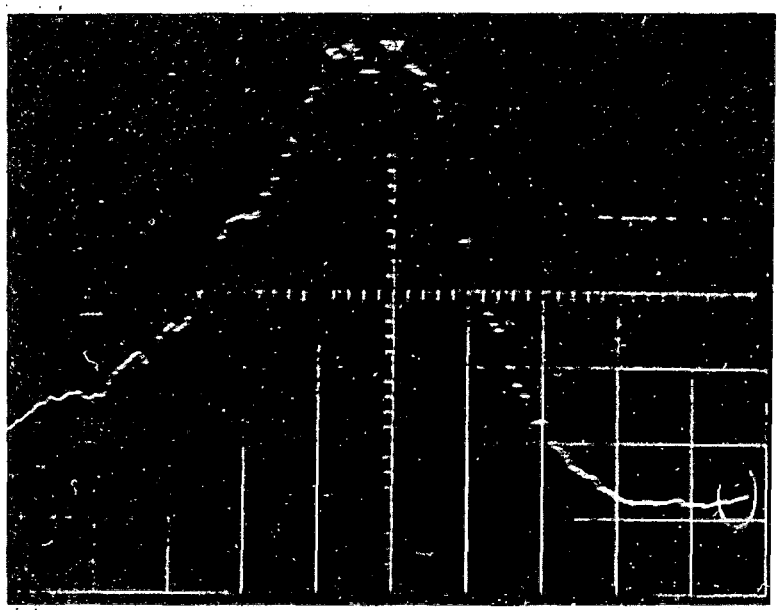

XBB 7210-5370

Fig. 2

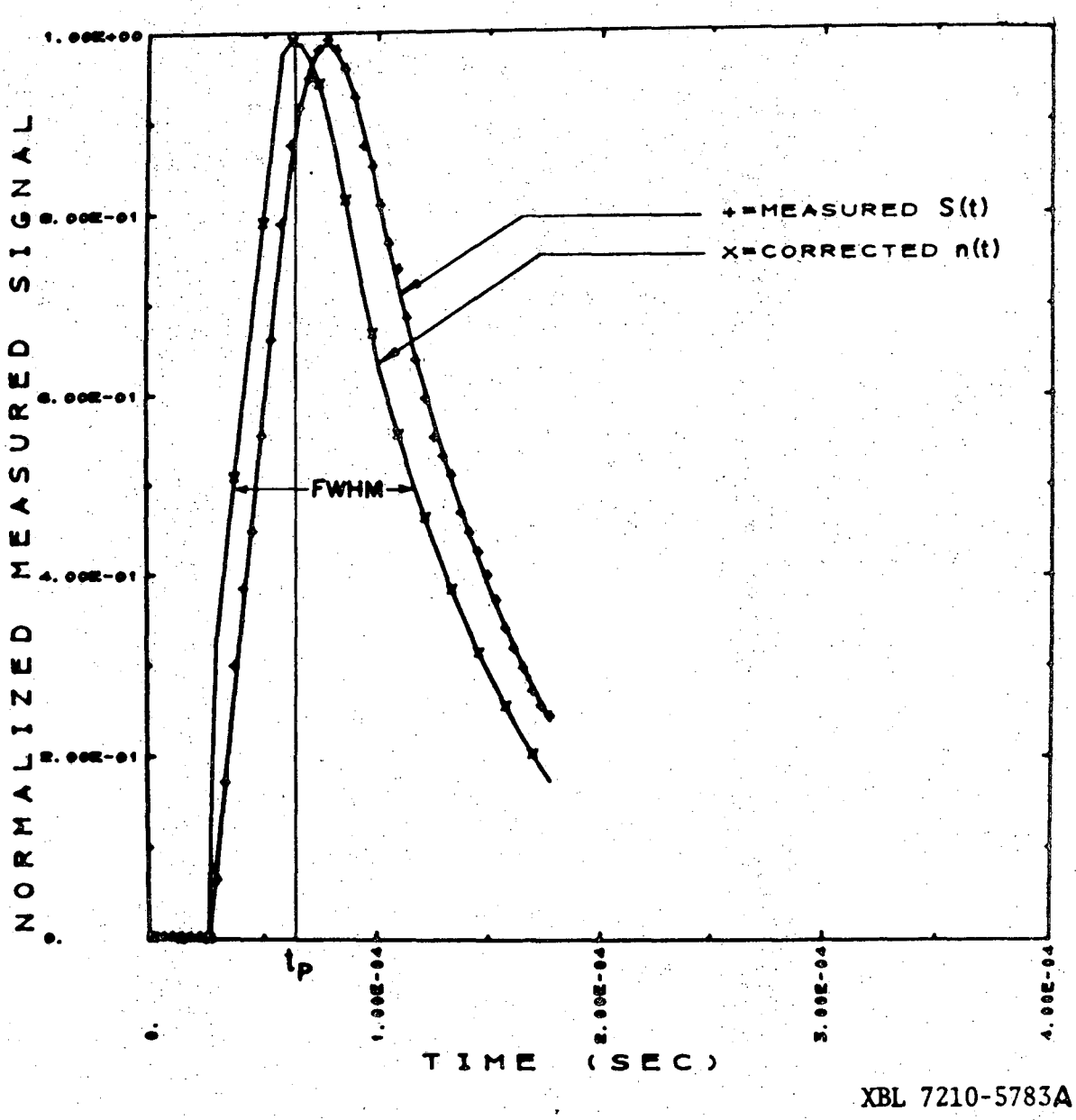
NORMALIZED MEASURED SIGNAL
1.00E+00
8.00E-01
6.00E-01
4.00E-01
2.00E-01
0.
+=MEASURED S(t)
X=CORRECTED n(t)
FWHM
t_p
0.
1.00E-04
2.00E-04
3.00E-04
4.00E-04
TIME (SEC)
XBL 7210-5783A

Fig. 3

0 0 0 0 4 2 0 1 4 0 8

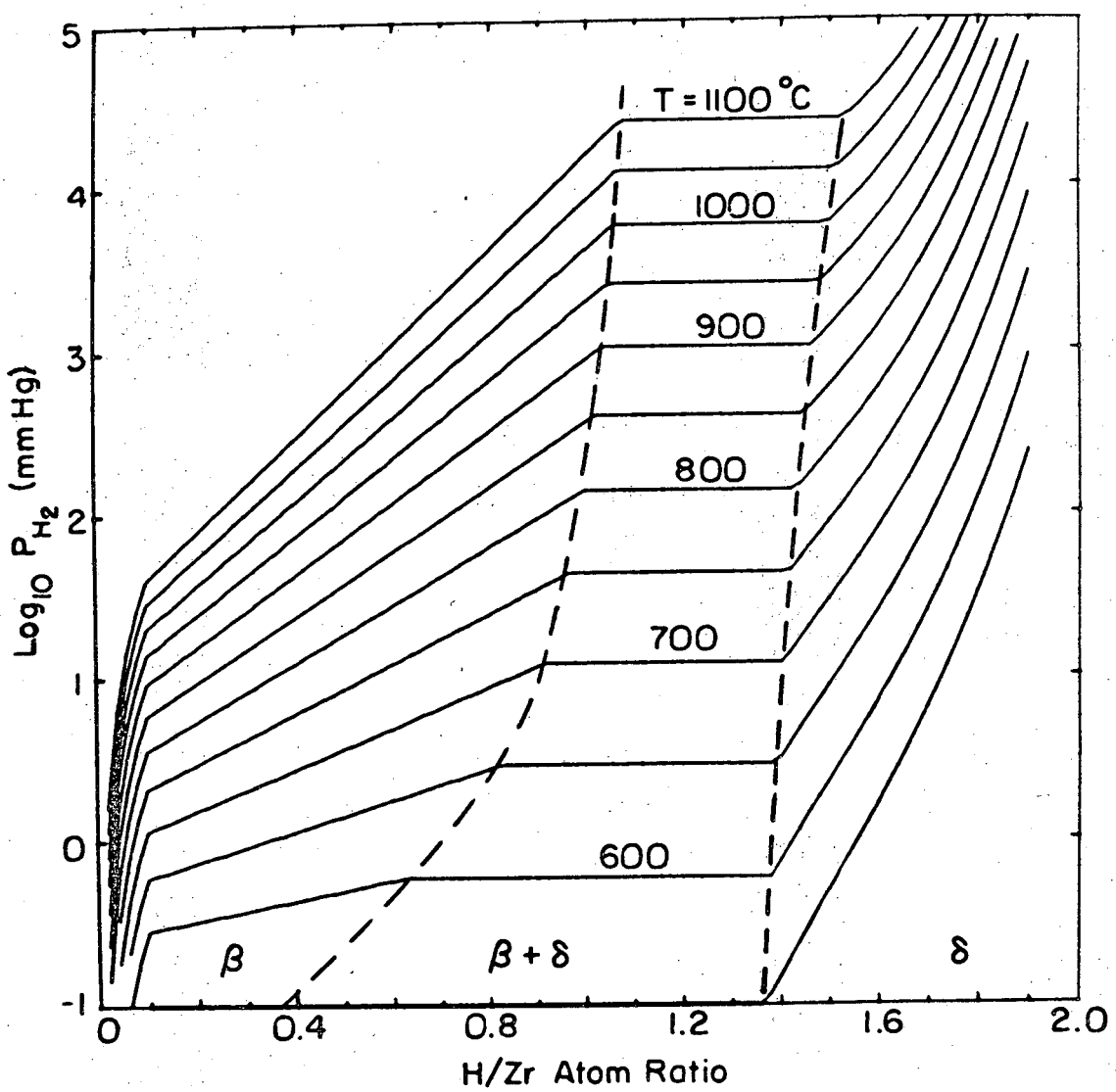

XBL 7210-5778

Fig. 4

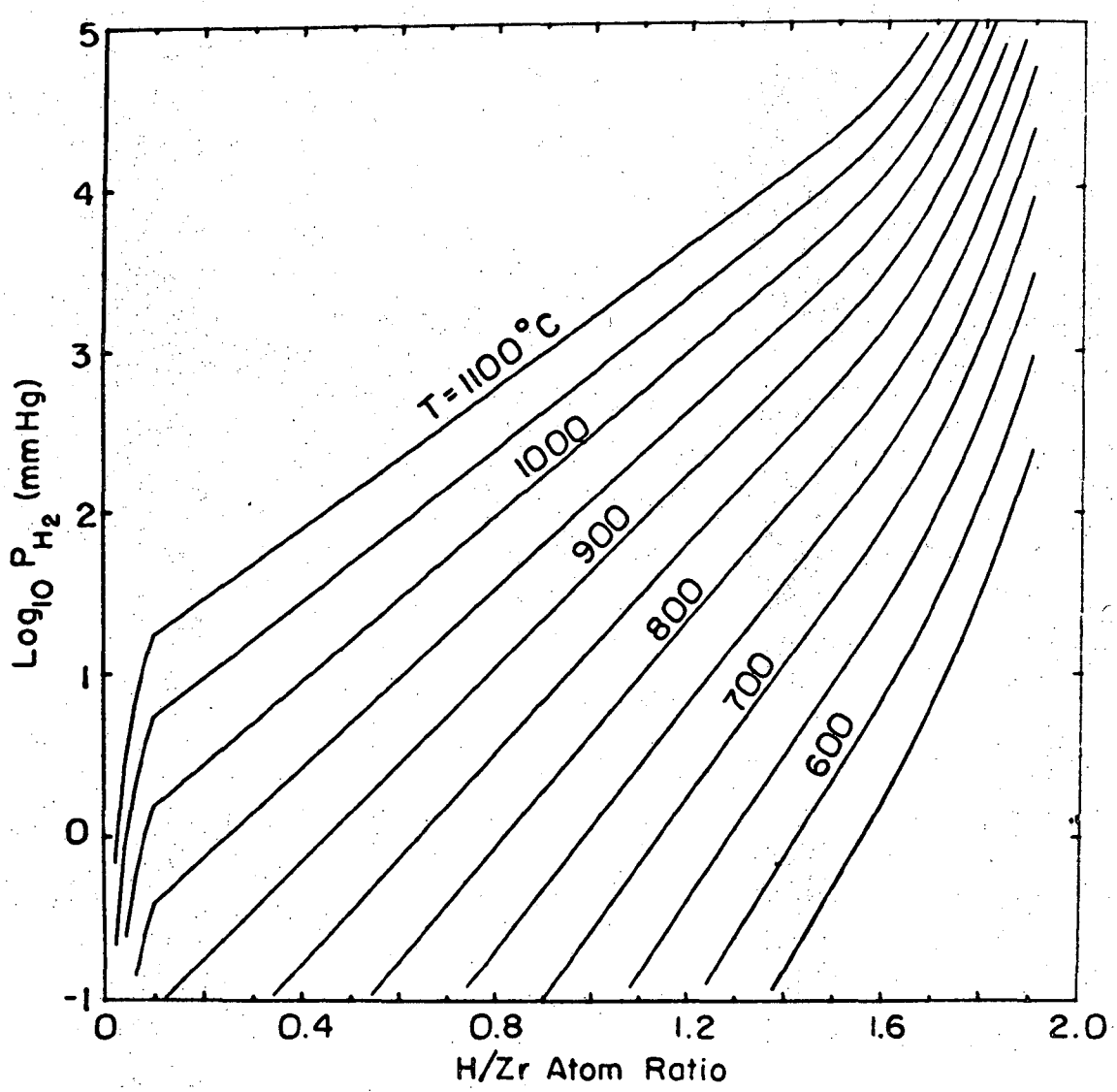

XBL 7210-5780

Fig. 5

0 0 0 0 4 2 0 1 4 0 9

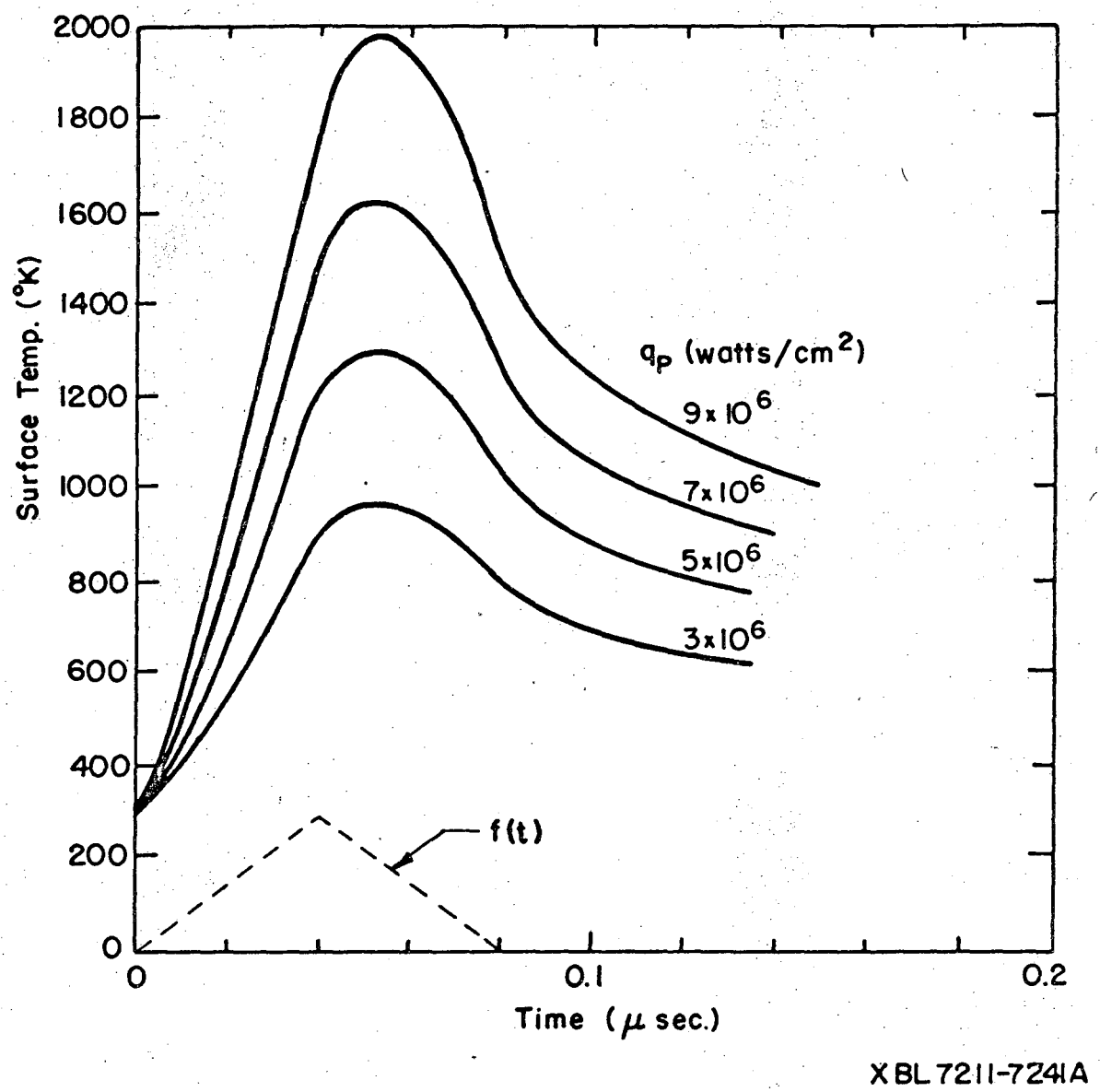

Fig. 6

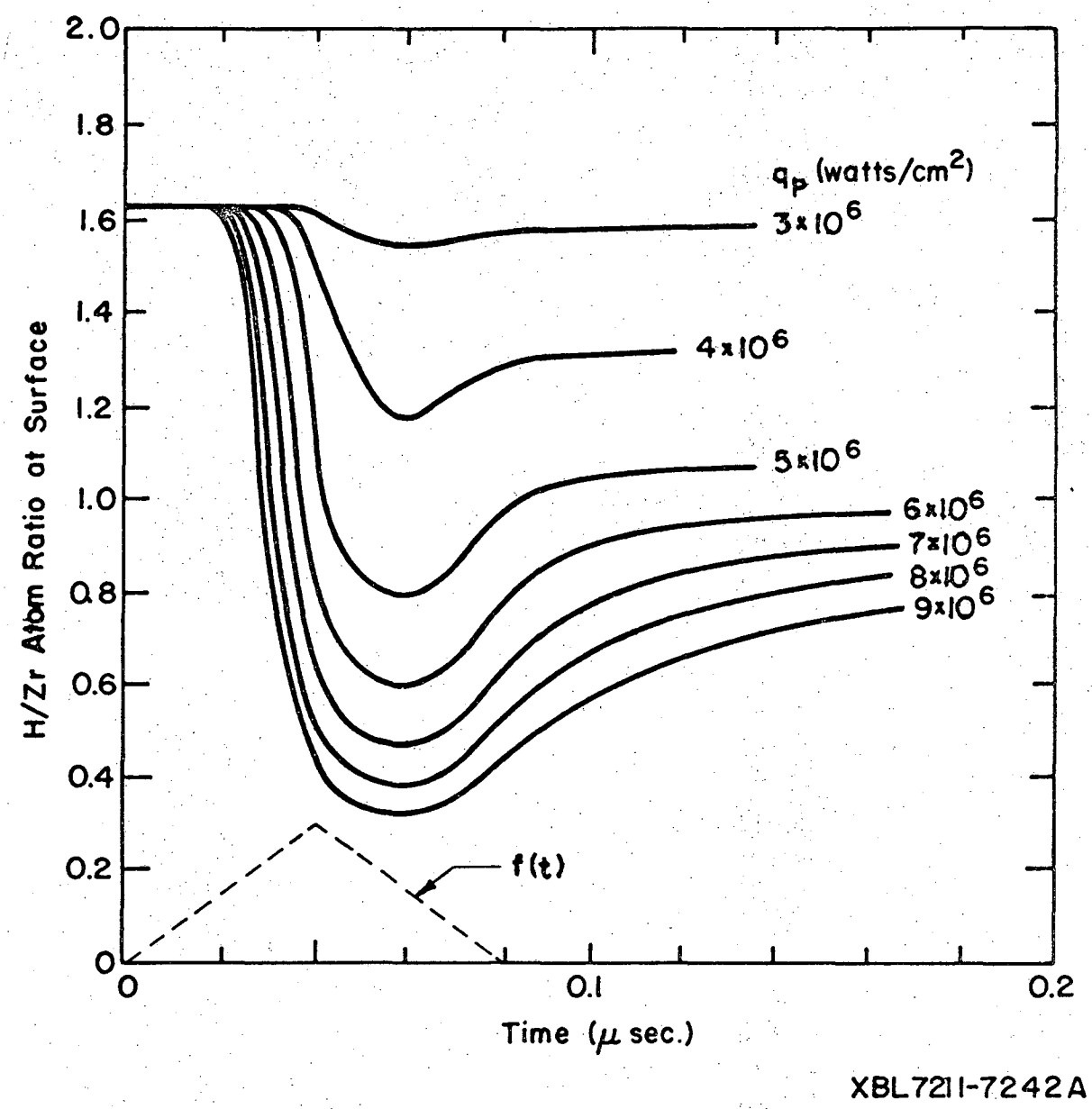
2.0
1.8
1.6
1.4
1.2
1.0
0.8
0.6
0.4
0.2
0
H/Zr Atom Ratio at Surface
q_p (watts/cm^2)
3×10^6
4×10^6
5×10^6
6×10^6
7×10^6
8×10^6
9×10^6
f(t)
0
0.1
0.2
Time (μ sec.)
XBL7211-7242A

Fig. 7

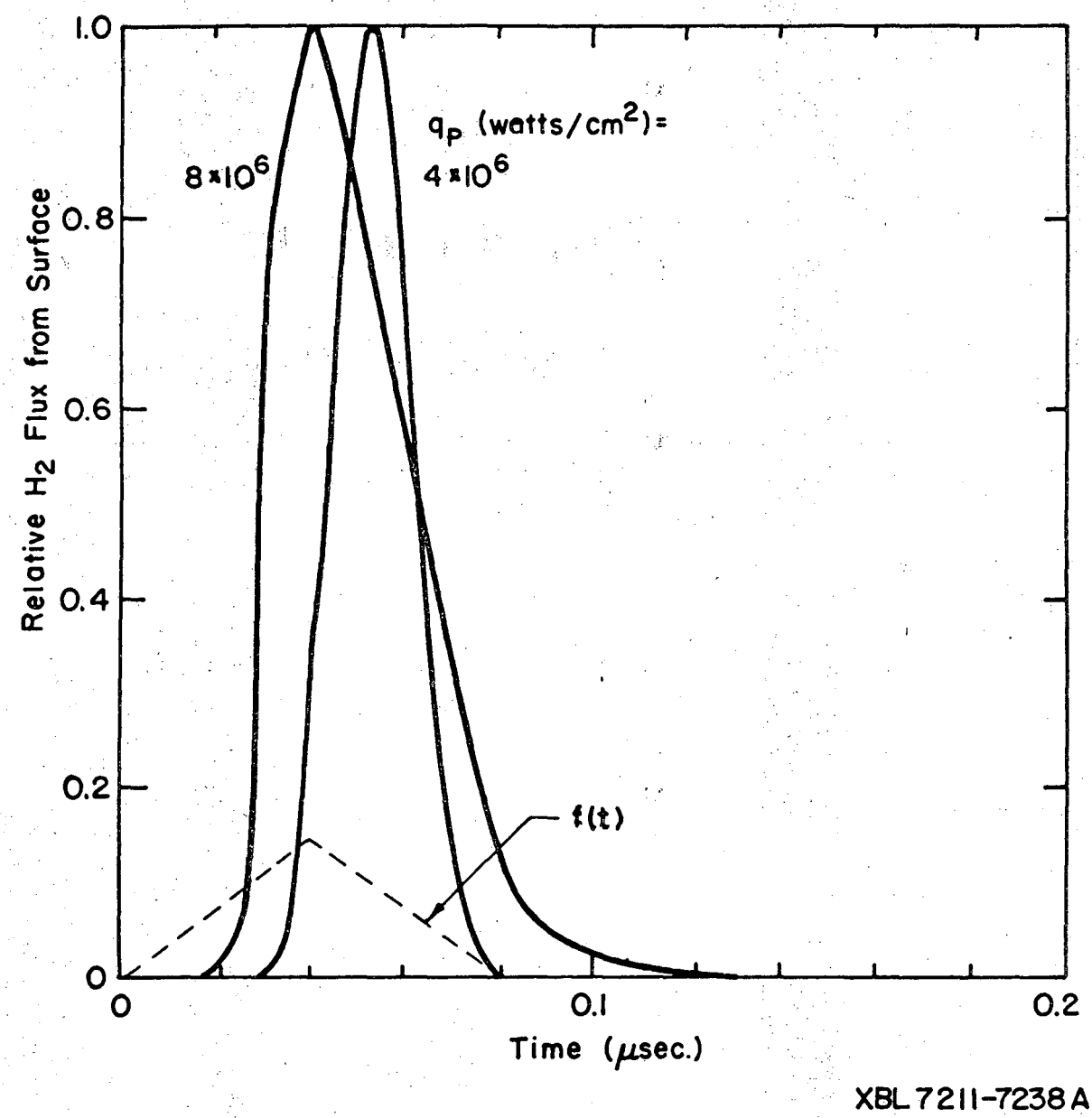
1.0
0.8
0.6
0.4
0.2
0
Relative H_2 Flux from Surface
q_p (watts/cm^2)=
8×10^6
4×10^6
f(t)
0
0.1
0.2
Time (μsec.)
XBL 7211-7238 A

Fig. 8

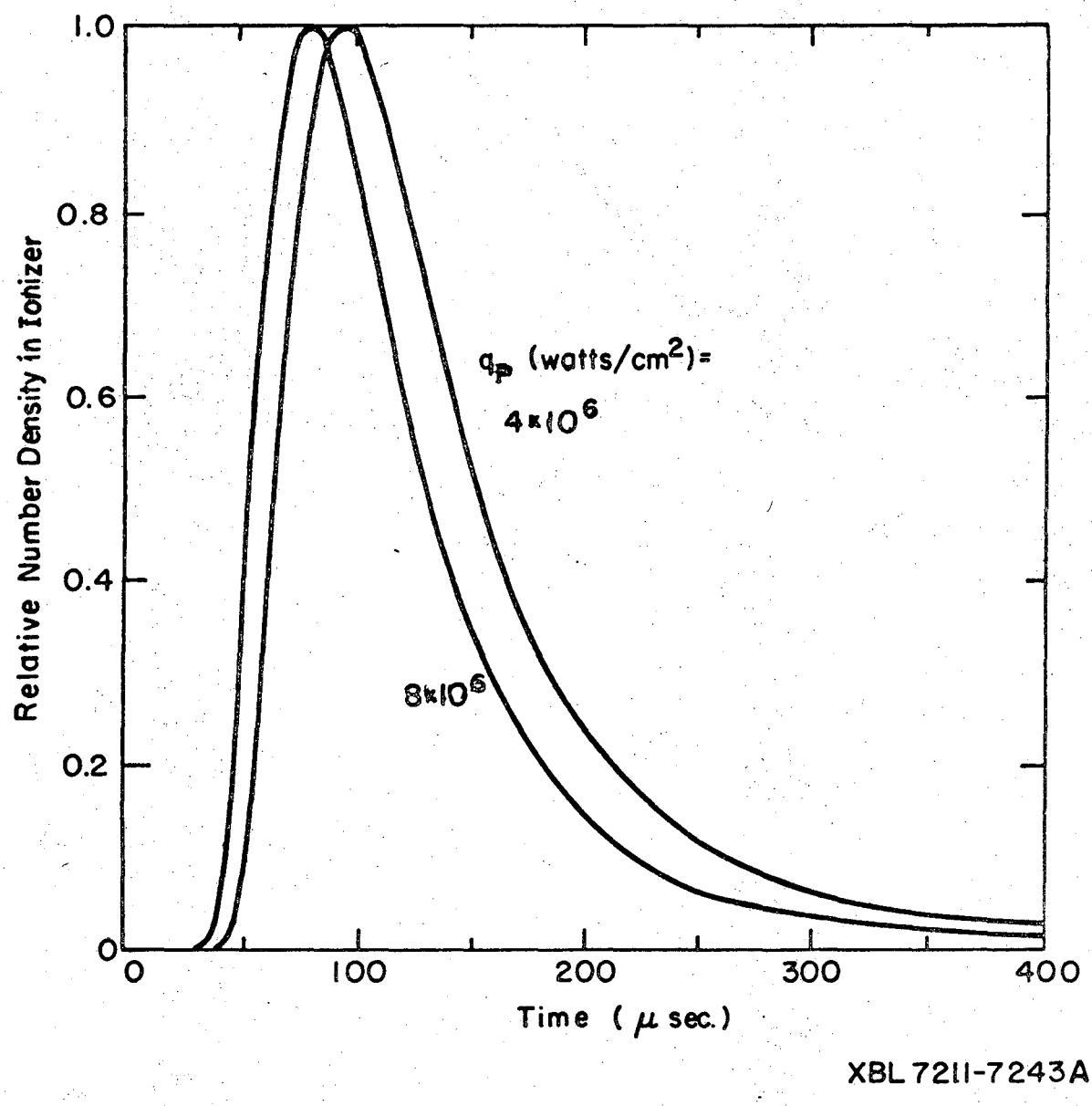
1.0
0.8
0.6
0.4
0.2
0
Relative Number Density in Ionizer
q_p (watts/cm^2)=
4×10^6
8×10^6
0
100
200
300
400
Time (μ sec.)
XBL 7211-7243A

Fig. 9

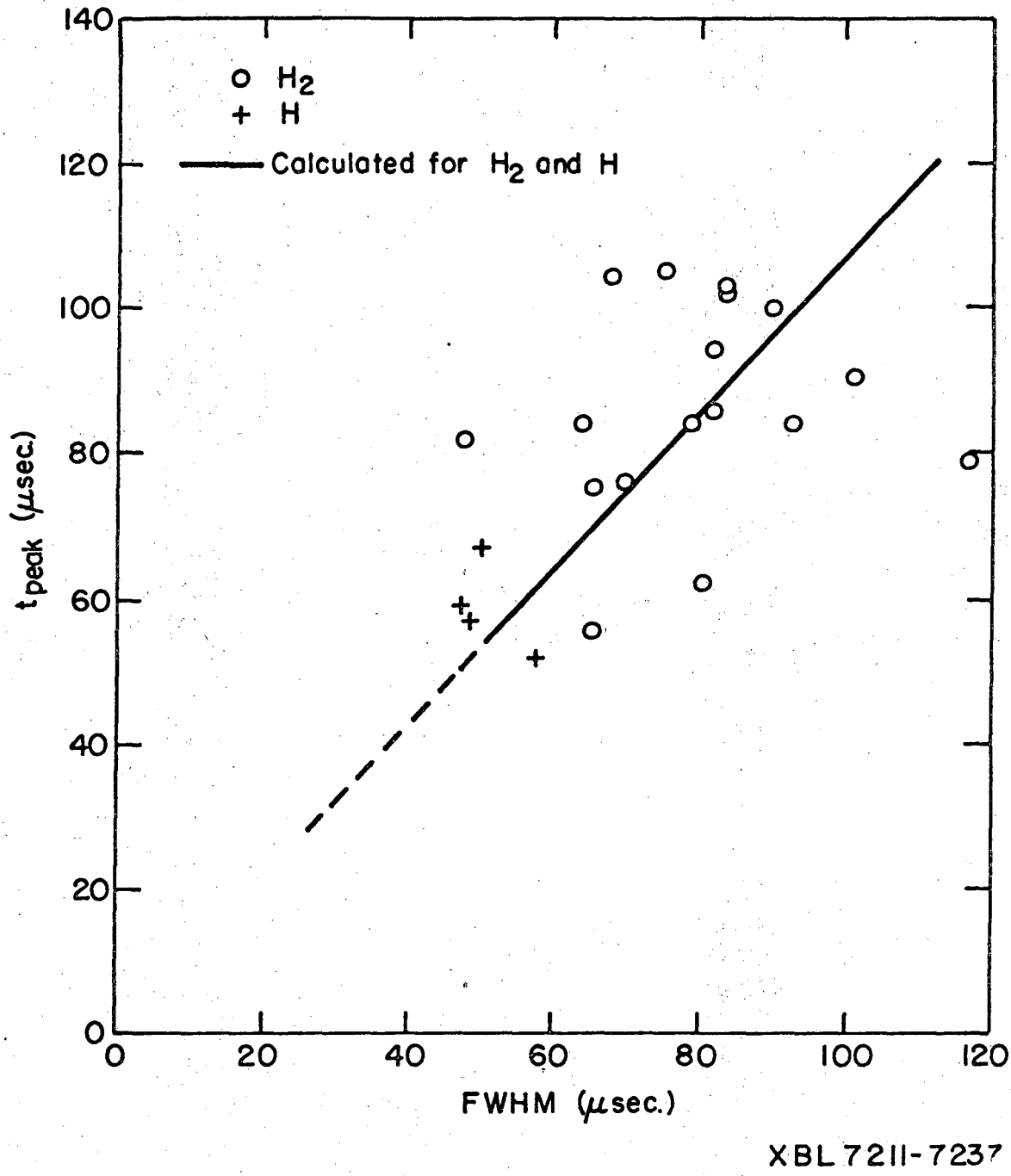
o H2
+ H
Calculated for H2 and H
140
120
100
80
60
40
20
0
0
20
40
60
80
100
120
t peak (μsec.)
FWHM (μsec.)
XBL 7211-7237

Fig. 10

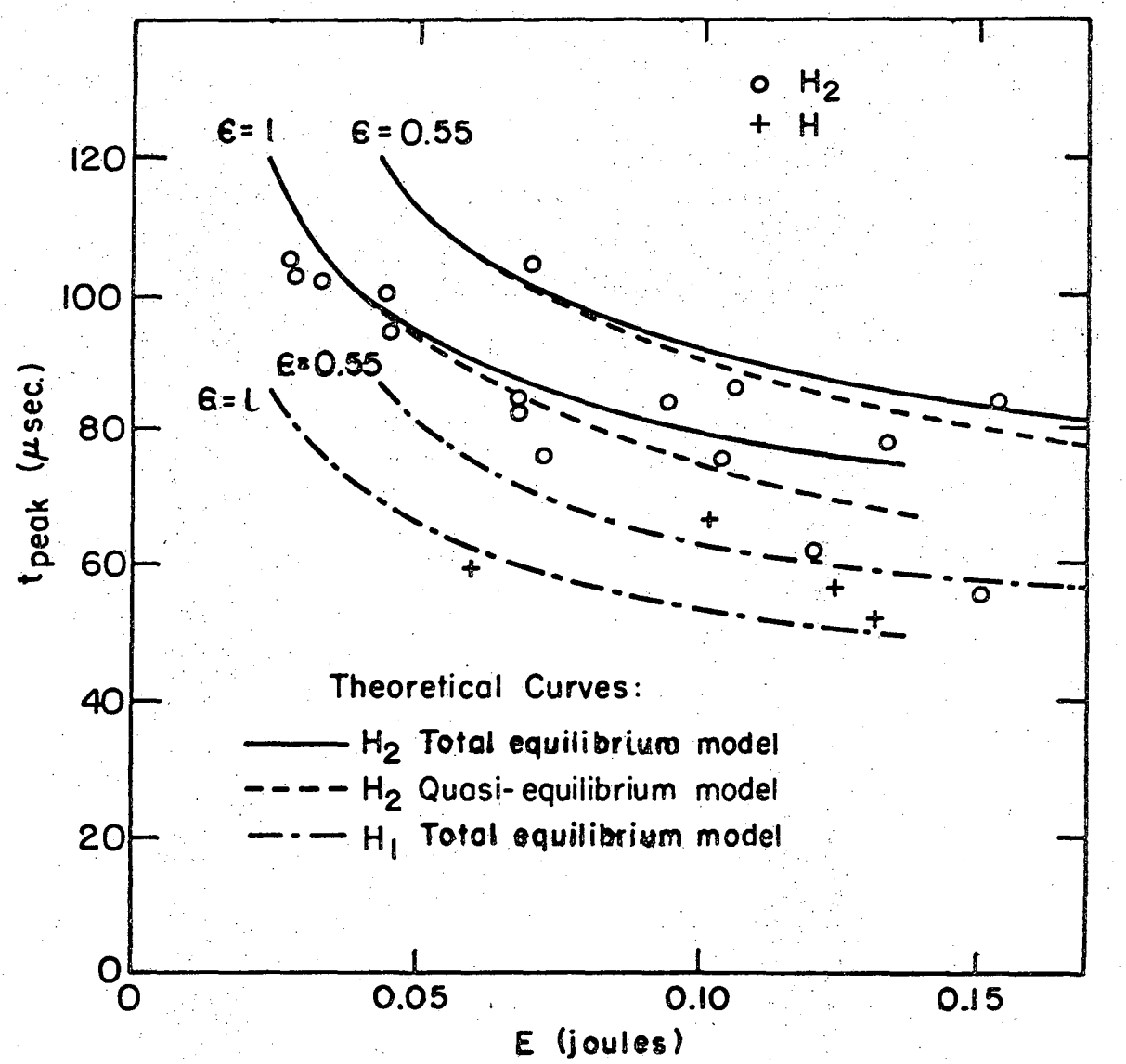

XBL 7211-7234 A

Fig. 11

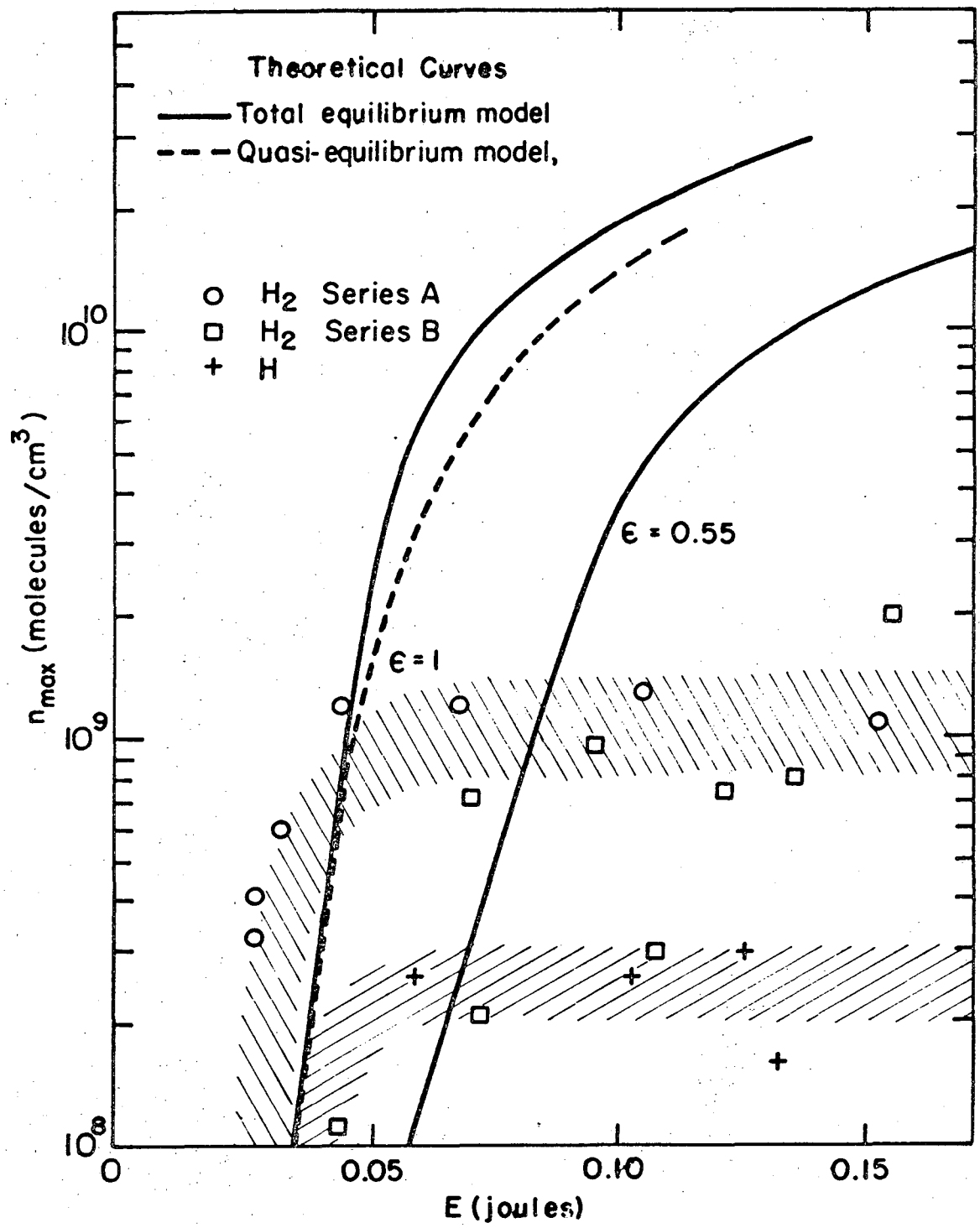

XBL 7211-7233 A

Fig. 12

0 0 0 0 4 2 0 1 4 1 2

LEGAL NOTICE

This report was prepared as an account of work sponsored by the United States Government. Neither the United States nor the United States Atomic Energy Commission, nor any of their employees, nor any of their contractors, subcontractors, or their employees, makes any warranty, express or implied, or assumes any legal liability or responsibility for the accuracy, completeness or usefulness of any information, apparatus, product or process disclosed, or represents that its use would not infringe privately owned rights.

TECHNICAL INFORMATION DIVISION
LAWRENCE BERKELEY LABORATORY
UNIVERSITY OF CALIFORNIA
BERKELEY, CALIFORNIA 94720